Identification of the λ integrase surface that interacts with Xis reveals a residue that is also critical for Int dimer formation

David Warren*[†], My D. Sam*[†], Kate Manley*[†], Dibyendu Sarkar[§], Sang Yeol Lee*, Mohamad Abbani[‡],
Jonathan M. Wojciak[‡], Robert T. Clubb[‡][¶], and Arthur Landy*[¶]

*Division of Biology and Medicine, Brown University, Providence, RI 02912; [‡]Department of Chemistry and Biochemistry, Molecular Biology Institute,
University of California, and UCLA–DOE Institute for Genomics and Proteomics, 405 Hilgard Avenue, Los Angeles, CA 90095; and [§]Institute of
Microbial Technology, Sector 39A, Chandigarh 160036, India

Lambda integrase (Int) is a heterobivalent DNA-binding protein
that together with the accessory DNA-bending proteins IHF, Fis,
and Xis, forms the higher-order protein–DNA complexes that
execute integrative and excisive recombination at specific loci on
the chromosomes of phage λ and its *Escherichia coli* host. The large
carboxyl-terminal domain of Int is responsible for binding to
core-type DNA sites and catalysis of DNA cleavage and ligation
reactions. The small amino-terminal domain (residues 1–70), which
specifies binding to arm-type DNA sites distant from the regions of
strand exchange, consists of a three-stranded β-sheet, proposed to
recognize the cognate DNA site, and an α-helix. We report here
that a site on this α-helix is critical for both homomeric interactions
between Int protomers and heteromeric interactions with Xis. The
mutant E47A, which was identified by alanine-scanning mutagen-
esis, abolishes interactions between Int and Xis bound at adjacent
binding sites and reduces interactions between Int protomers
bound at adjacent arm-type sites. Concomitantly, this residue is
essential for excisive recombination and contributes to the effi-
ciency of the integrative reaction. NMR titration data with a
peptide corresponding to Xis residues 57–69 strongly suggest that
the carboxyl-terminal tail of Xis and the α-helix of the amino-
terminal domain of Int comprise the primary interaction surface for
these two proteins. The use of a common site on λ Int for both
homotypic and heterotypic interactions fits well with the complex
regulatory patterns associated with this site-specific recombina-
tion reaction.

The bacteriophage λ-encoded integrase (Int) belongs to a
subgroup of the tyrosine recombinase family known as the
heterobivalent recombinases (1, 2). These recombinases catalyze
reactions that are distinguished from other pathways of site-
specific rearrangement and movement of DNA by their direc-
tionality. This feature is built on the ability of these recombinases
to simultaneously bind and bridge two distinct and well sepa-
rated DNA-binding sites (3–5). Int binds with high affinity to
arm-type DNA sites by means of a small amino-terminal domain
(residues 1–70) whereas it binds with lower affinity to core-type
sites by means of a larger carboxyl-terminal domain (residues
75–356), which also executes DNA strand cleavage and ligation.
Bridging between arm and core sites is facilitated by DNA bends
induced by accessory proteins (IHF, Xis, and Fis) bound to DNA
sites located between the arm- and core-type sequences (5–9).
This ensemble of DNA-bending- and DNA-bridging-proteins
forms the large recombinogenic complexes that confer direc-
tionality on the recombination reaction. In this article we show
that formation of both the Int–Xis and Int–Int complexes, key
elements in the structure and function of the higher-order
recombinogenic structures, depends on a common site in the
amino-terminal domain of Int.

The λ Int recombinase catalyzes the integration and excision
of viral DNA into and out of the chromosome of its *Escherichia
coli* host (10, 11). The product of recombination between viral

attP (POP′) and bacterial attB (BOB′) sites is an integrated
prophage bounded by hybrid att sites, attL (BOP′) and attR
(POB′), which are themselves substrates for excisive recombi-
nation (Fig. 1). The strand nicking and joining events take place
at the core sites within a synaptic higher-order structure that
brings together two core regions bound by an Int tetramer.
Recombination proceeds by means of an ordered pair of trans-
esterification reactions that first generate and then resolve a
Holliday junction recombination intermediate (Fig. 1; refs. 12
and 13). This mechanism comprises the hallmark for the tyrosine
recombinase family.

For the heterobivalent recombinases there is an overlay of
additional complexity that is to be found in the phage DNA
sequences (P and P′) flanking the core region in attP and
distributed to each of the prophage att sites (BOP′ and POB′).
Encoded within these DNA sequences are the five arm-type
Int-binding sites and the six sites for the accessory DNA-bending
proteins, as diagrammed in Fig. 1. Two overlapping subsets of this
ensemble are used for integrative and excisive recombination (8,
14). This complexity facilitates the unique directional control of
recombination that is characteristic of λ Int and related hetero-
bivalent recombinases.

Critical insight into the mechanisms of recombination has
been provided by crystal and NMR structures of Int family
members (15–20) and each of the individual elements of the λ
intasome. These include x-ray crystal structures of Fis protein
(21–23), IHF bound to its cognate DNA site (24), the unliganded
catalytic domain of λ (25), the DNA-liganded carboxyl-terminal
domain of λ (26) and the NMR structures of the amino-terminal
domains of Int (27) and Xis (28). As a step toward understanding
how these structures fit and function together, we describe the
interactions of the amino-terminal domain of Int with itself and
with Xis.

The first 50 residues of Xis adopt a winged-helix structure that
is thought to be responsible for DNA binding at the X1 and X2
sites on attR (28). The carboxyl-terminal residues (52–72), which
are disordered in the absence of DNA, are required for inter-
action with Int bound at the adjacent P2 site (28–30). The
amino-terminal domain of Int, consisting of a three-stranded
β-sheet and an α-helix, is proposed to recognize its cognate DNA
arm sites through the three-stranded β-sheet (27). In addition to
binding five arm-type DNA sites, it interacts with Xis when the
two proteins are bound at P2 and X1, respectively, and interacts
with itself when bound to the P′1,2,3 arm-type sites (Fig. 1). We
now show that the α-helix within the amino-terminal domain of
Int is critical for both the homomeric interactions between Int
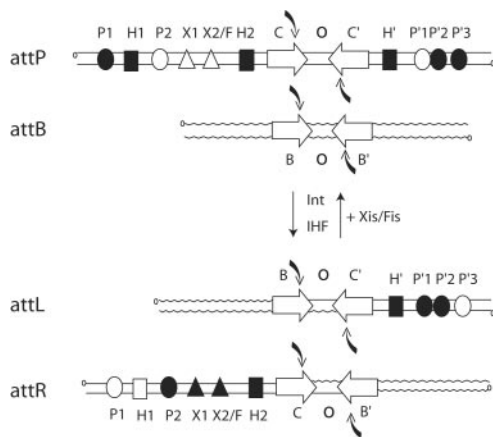

Fig. 1. Location and occupancy of protein-binding sites during integrative and excisive recombination. Integrative recombination between the phage *att*P and bacterial *att*B sites requires the phage-encoded Int protein and the host-encoded IHF to generate the *att*L (*Left*) and *att*R (*Right*) prophage sites. Excisive recombination between *att*L and *att*R additionally requires the phage-encoded Xis protein and is assisted by the host-encoded Fis protein. Protein-binding sites in the arms of *att*P, *att*L, and *att*R that are occupied during integration and excision are shown as filled symbols. Int has four core-type sites (C, C′, B, and B′) that flank the 7-bp overlap region (O) as inverted repeats (inverted open arrows) and encompass each of the DNA-cleavage sites (curved filled arrows). There are five arm-type Int-binding sites (circles): two single sites in the P arm (P1 and P2) and three adjacent sites in the P′ arm (P′1, P′2, and P′3). IHF has three binding sites, H1, H2, and H′ (squares), and Xis has two binding sites, X1 and X2 (triangles), one of which (X2) overlaps with the single Fis-binding site (F).

protomers and the heteromeric interactions with Xis, and that a 13-residue peptide from the carboxyl-terminal portion of Xis specifically interacts with residues on one face of this α-helix.

Materials and Methods

Oligonucleotides and Mutagenesis. The coding region of Xis was cloned into the pET-16b expression vector (Novagen). The single-point mutations E47A and R30D of Int and R63E of Xis were cloned into their relevant expression vectors (27, 31) by using the QuikChange site-directed mutagenesis kit (Stratagene) with the following SDS/PAGE-purified oligonucleotides (Operon Technologies, Alameda, CA): (*i*) E47A 5′-GAATCG-CAATCACTGCGGCTATACAGGCC-3′; (*ii*) R30D 5′-CTG-CTACAGGGACCCAGACACGGGTAAAGAGTTTGG; (*iii*) R63E 5′-GGCCTTTTGAAGGAGATCAGAAATGGG-3′; and their corresponding complementary strands. HPLC-purified substrate oligonucleotides were 5′ end-labeled with ^{32}P by the use of phage T4 polynucleotide kinase (32) and were separated from free label by using a Biospin P-30 chromatography column (Bio-Rad). Sequences of the top strands for each of the double-stranded oligonucleotides used in this work are as follows (with Int- and Xis-binding sites denoted as bold caps): (*i*) 40-bp P2X1 5′-TAGGATTC**ATAGTGACTG**C**ATATGTTGTGTTTT**C-GAGATG-3′; and (*ii*) 50-bp P′1,2 5′-CATTGCTCAACGA-AC**AGGTCACTATCAGTCAAAAT**TTGATTTCATACCAT-3′.

Protein Expression and Purification. Proteins were produced in *E. coli* BL21(DE3)pRIL from expression plasmids under the control of the T7 promoter. Int proteins were purified to near homogeneity as described (27, 31, 33, 34). Cells expressing the Met-Gly-(His)$_{10}$-(Ser)$_2$-Gly-His-Ile-Glu-Gly-Arg-His-Xis fusion protein were resuspended in potassium phosphate buffer (50 mM KPO$_4$, pH 8.0/10% glycerol/1 M NaCl/2 mM DTT/2 mM EDTA, pH 8.0/1 mM benzamidine/1 mM phenylmethanesul-

fonyl fluoride). The sonicated extracts were centrifuged at 12,000 × *g* for 30 min at 4°C to remove insoluble material and further purified through polyethylene glycol (PEG) precipitation (4°C, 1 h) by using one-fifth volume potassium phosphate buffer containing PEG-8000 [30% (wt/vol)] and further clarified by centrifugation at 12,000 × *g* for 30 min at 4°C. An equal volume of potassium phosphate buffer without any NaCl was added to the soluble extract to lower the NaCl concentration to 500 mM before fractionation by phosphocellulose column chromatography. After extensive stepwise washing with potassium phosphate buffers containing NaCl at concentrations ranging from 0.5 to 1.6 M, the proteins were eluted off the column in potassium phosphate buffer containing 2.2 M salt and subsequently concentrated with Gelman filters. The concentrations of all proteins were estimated by the dye-binding method by using bicinchoninic acid (Pierce) (35, 36). The purity of all of the proteins was >90% as judged by Coomassie blue staining of overloaded SDS/polyacrylamide gels.

Gel Retardation Assays. Binding of Xis or Int to double-stranded DNA fragments was carried out in 10 mM Tris·HCl (pH 7.5)/75 mM NaCl/0.5 mg/ml BSA/1 mM EDTA/20 ng/μl sheared herring sperm DNA/2.5 mM DTT, and with the indicated concentrations of radiolabeled DNA. In all DNA-binding experiments the proteins were mixed with DNA in the binding mix and incubated for 30–40 min at 25°C. The reactions were analyzed by electrophoresis (100 V for 4–6 h) through native, nondenaturing 8% (wt/vol) polyacrylamide gels. Each dried gel was visualized by autoradiography and phosphorimaging. The amounts of free and bound DNA were quantified with a PhosphorImager and MACBAS-2500 image analysis software (Fuji).

Recombination Assays. Recombination reactions were carried out in Tris recombination buffer [0.45 μg of linear *att*L or *att*B per assay, 0.3 μg of supercoiled *att*R or *att*P per assay, 5 mM EDTA (pH 8.0), 6 mM spermidine, 25 mM Tris (pH 8.0), 0.5 mg/ml BSA, 2.5 mM DTT, 30 mM NaCl, and 2 units of IHF per assay]. For excisive recombination reactions the buffer was further supplemented with 0.6 μM Xis. In all experiments, Int proteins were mixed with the DNA in the assay mix and incubated for 2–4 h at 25°C. The reactions were stopped by the addition of SDS-containing buffer and analyzed by electrophoresis (100 V for 3–4 h) through 1.2% agarose gels in Tris-acetate-EDTA buffer. Imaging and quantitation were performed as per the gel retardation assays.

NMR Studies. A peptide containing residues 1–64 of Int (INT-DBD$^{1-64}$) was uniformly enriched with nitrogen-15 and purified to homogeneity as described (27). NMR studies made use of an ≈1.1 mM sample of ^{15}N INT-DBD$^{1-64}$ dissolved in titration buffer [40 mM NaOAc, pH 5.5/80 mM NaCl/10 mM deuterated DTT (90% H$_2$O:10% D$_2$O)]. A 13-mer peptide corresponding to residues 57–69 of ^{λ}Xis (TGGLLKRIRNGKK) was purchased from Genemed Synthesis (South San Francisco, CA) and purified by reverse-phase HPLC. The peptide was then lyophilized and dissolved in titration buffer (final peptide concentration of 11 mM). ^{1}H–^{15}N HSQC NMR spectra of the ^{15}N INT-DBD$^{1-64}$ protein were recorded after the addition of various amounts of peptide (protein:peptide ratios: 1:0, 1:1, 1:1.5, 1:2, 1:3, 1:5, and 1:10). Backbone amide resonances were assigned by monitoring changes in the ^{1}H–^{15}N HSQC spectrum of the free protein after the addition of peptide. NMR data were acquired by using a Bruker (Billerica, MA) DRX-600 MHz spectrometer, and processed and analyzed by using the programs NMRPIPE (37) and NMRVIEW (38), respectively. The model was constructed by manually docking the structures of ^{15}N INT-DBD$^{1-64}$ (27) and $^{1-55}$Xis^{C28S} (residues 1–55 of the λ excisionase protein with a
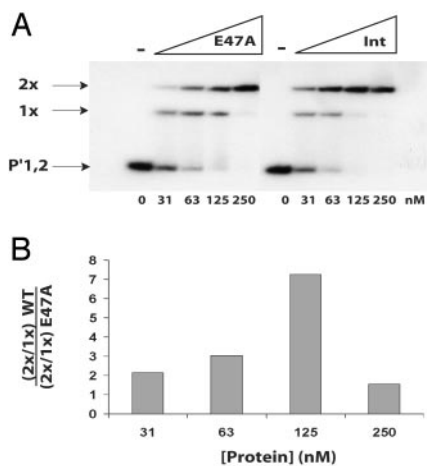
Fig. 2. Residue E47 is required for intermolecular Int–Int interactions. (*A*) Int proteins were tested in a gel-shift assay for their abilities to bind to a 50-bp duplex containing the P'1,2 arm-type binding sites. The indicated concentrations of Int and E47A proteins were mixed with 2 nM radiolabeled DNA and incubated at 25°C for 30 min. Reactions were analyzed by electrophoresis on an 8% native polyacrylamide gel. The gels were then dried and visualized by autoradiography. (*B*) The intensity of the bands was measured as described in *Materials and Methods*. The ratio of the doubly bound species to the singly bound species has been calculated for both proteins, and the ratio of these values is plotted as a function of protein concentration.

cysteine-to-serine mutation at position 28; ref. 28) to B-form DNA by using the program MOLMOL (39).

Results

Residue E47 Is Required for Intermolecular Int–Int Interactions. Previous studies (27) on the amino-terminal domain of Int implicated the three-stranded β-sheet in arm-site DNA binding while the function of the amino-terminal α-helix remained unknown. To probe the function of the α-helix we performed an alanine-scanning mutagenesis (residues 40–55) and tested each of the mutant proteins for binding to an arm-type DNA site adjacent to a second arm-type site or to a Xis-binding site. The mutations were initially tested in the context of an isolated amino-terminal domain (N1–75). This procedure aided purification and eliminated complications from protein–protein interactions known to be associated with the much larger carboxyl-terminal domain. The N1–75 fragment has already been shown to be a good model for the amino-terminal functions of full-length Int (40).

Of the 18 residues in the α-helix, six were not changed; three alanines at positions 44, 48, and 51, and the three carboxyl-terminal residues at positions 56–58. The I49A mutation was not recovered and the N52A mutation had no DNA-binding activity at all, and therefore could not be distinguished from a misfolded protein. Of the remaining mutants, E47A showed the largest difference from the wild-type protein in both Int–Int and Int–Xis binding assays and it was therefore constructed in the context of full-length Int.

As reported (40), wild-type Int binds cooperatively to a radiolabeled 50-bp duplex containing the P'1,2 arm-type sites to yield singly bound and doubly bound complexes (Fig. 2*A*) that are appropriately retarded in electrophoretic mobility shift assays. Whereas the E47A mutant binds single arm-type sites as well as does wild-type Int (Fig. 2*A*), it is clearly less efficient in forming the doubly bound complex (Fig. 2*A*). The difference between the wild-type and mutant proteins in their respective ability to form the doubly bound complex is most apparent at 125 nM as the amount of total binding to the substrate approaches 100% (Fig. 2*B*).
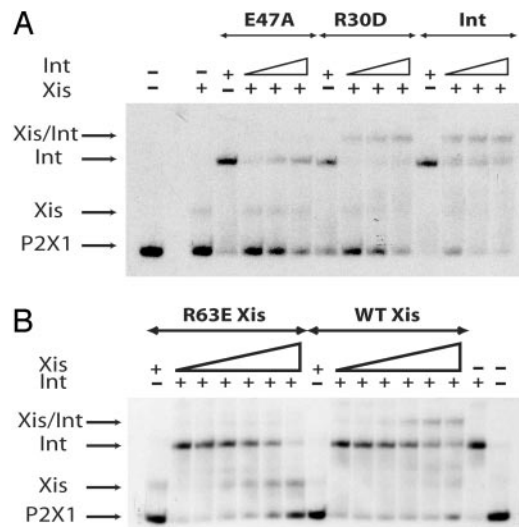

Fig. 3. Residues E47 of Int and R63 of Xis are required for Int–Xis–DNA ternary complex formation. Proteins were tested in a gel-shift assay for their respective abilities to bind to a 40-bp duplex containing the P2X1 binding sites. (*A*) The substrate DNA (2 nM) was preincubated at 25°C for 10 min with Xis (850 nM). Wild-type, E47A, or R30D Ints (500 nM) were then added to the first tube, followed by two serial 2-fold dilutions and the reactions incubated at 19°C for 30 min. (*B*) The substrate DNA (2 nM) was preincubated at 25°C for 10 min with Int (118 nM). Wild-type or R63E Xis proteins (600 nM) were added to the first tube followed by two serial 2-fold dilutions and the reactions incubated at 19°C for 30 min. For all three panels, reactions were analyzed by electrophoresis on 8% native polyacrylamide gels. The gels were then dried and visualized by autoradiography.

Residues E47 of Int and R63 of Xis Are Required for Int–Xis–DNA Complex Formation. Having shown that E47A is defective in homotypic dimer formation on adjacent arm-type sites, we tested cooperative binding of E47A and Xis to their respective, adjacent P2 and X1 sites (Fig. 3*A*). Because R63 had been previously implicated in cooperative interactions with Int (30) we also tested the R63E mutant of Xis (Fig. 3*B*).

When a 40-bp duplex containing the adjacent P2 and X1 target sites is incubated with Xis or Int alone, single retarded bands are observed with relative mobilities consistent with the difference in size between the two proteins (Fig. 3). Presence of both Int and Xis yields a third band that migrates more slowly than with Int or Xis bound alone (Fig. 3) and is consistent with previous work (40). The formation of this ternary complex is dramatically reduced if either E47A Int (Fig. 3*A*) or R63E Xis (Fig. 3*B*) is used. Because both mutant proteins are able to form singly bound complexes on their respective target sites (Fig. 3), their defects are presumably in the protein–protein interactions involved in ternary complex formation. For reasons described below, we also tested another Int mutant, R30D, which was found to be superior to wild-type Int in the formation of ternary complexes with Xis, relative to Int binding at P2, on the P2X1 DNA duplex (Fig. 3*A*).

E47 Plays a Role in Both Integrative and Excisive Recombination. To ascertain the consequences of the E47A defects on overall Int function, the mutant was compared with wild-type Int in integrative and excisive recombination reactions using radiolabeled linear *att*B or *att*L with supercoiled *att*P or *att*R substrates, respectively. E47A Int is virtually unable to execute excisive recombination in this assay at any concentration tested (Fig. 4*A*). It is also defective for integrative recombination. Although the total amount of product obtained with E47A after 4 h is
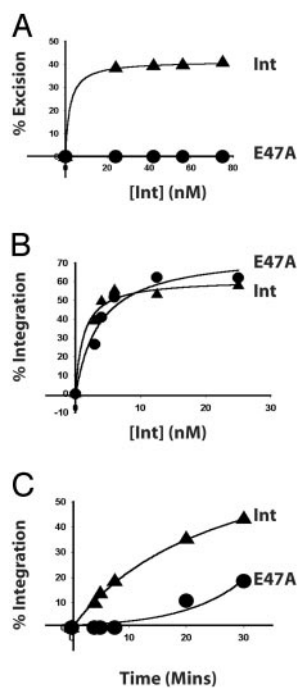
Warren *et al.*

Fig. 4. Residue E47 is required for both integrative and excisive recombination. Recombination reactions between supercoiled *att*R with radiolabeled, linear *att*L (*A*) and supercoiled *att*P with radiolabeled, linear *att*B (*B*) were carried out with IHF, Xis, and the indicated amounts of Int. (*C*) Kinetics of integrative recombination between supercoiled *att*P and radiolabeled, linear *att*B was determined with Int or E47A at 50 nM. The percent recombinant product is plotted as a function of protein concentration (*A* and *B*) or time (*C*).

comparable to that obtained with wild-type Int (Fig. 4*B*), the rate of recombination is clearly slower (Fig. 4*C*).

The Helix in INT-DBD$^{1-64}$ Interacts with Xis. Biochemical and genetic studies have suggested that the carboxyl-terminal tail of Xis directly contacts INT-DBD$^{1-64}$ because it is required for cooperative binding of Xis and INT-DBD$^{1-64}$ to sites P2 and X1 (29, 30, 41). In the absence of DNA, the carboxyl-terminal tail of Xis is unstructured and presumed to undergo a disordered-to-ordered transition in the INT-DBD$^{1-64}$–Xis–DNA ternary complex (28). To test whether this tail directly contacts INT-DBD$^{1-64}$, we performed a peptide titration study. We reasoned that INT-DBD$^{1-64}$ residues that form the Xis-interaction surface would exhibit large chemical shift changes when a peptide corresponding to the carboxyl-terminal tail of Xis (residues 57–69, TGGLLKRIRNGKK) is added. We acquired a series of ^{1}H–^{15}N HSQC NMR spectra of ^{15}N INT-DBD$^{1-64}$ with various amounts of the Xis peptide. The spectrum of the INT-DBD$^{1-64}$–peptide complex (1:10 protein-to-peptide ratio) is well resolved (Fig. 5*A*), enabling its resonances to be assigned and compared with the chemical shifts of the free form. Analysis of the data suggests that the peptide–INT-DBD$^{1-64}$ complex is in fast exchange on the chemical shift time scale, with a lifetime no greater than a millisecond (calculated from the maximum chemical shift change of 147 Hz for the amide ^{1}H of residue Leu-55). A peptide-to-protein ratio of 7.5:1.0 is required to saturate the complex, indicating that the peptide binds with very weak affinity ($K_D = \approx 3$ mM). Notably, the addition of the Xis peptide causes large and selective changes in the ^{1}H and ^{15}N backbone amide resonances of INT-DBD$^{1-64}$. The largest perturbations cluster to the carboxyl terminus of the single helix in INT-DBD$^{1-64}$ (residues 51–55), with more modest changes in adjacent residues (56–58), suggesting that this region of the protein
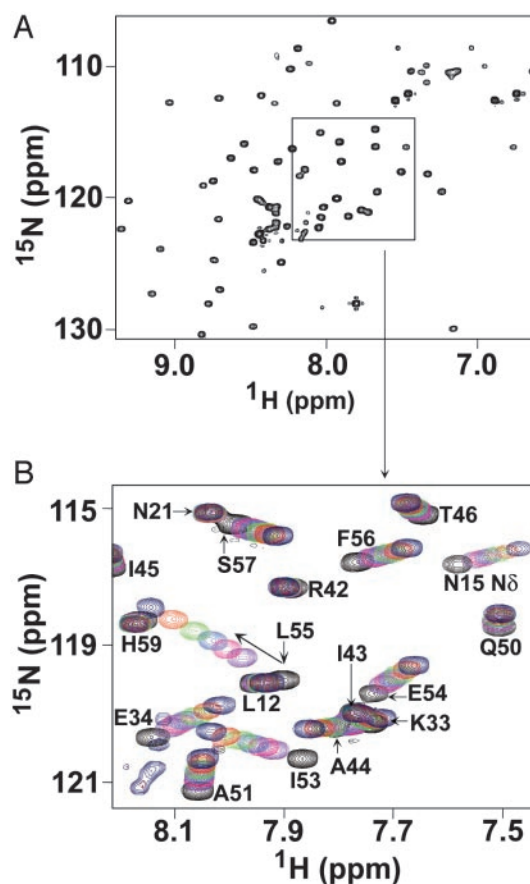

Fig. 5. The INT-DBD$^{1-64}$ and Xis proteins interact in solution. (*A*) The ^{15}N–^{1}H HSQC spectrum of the ^{15}N INT-DBD$^{1-64}$–Xis–peptide complex (1:10 protein-to-peptide ratio). The complex was in fast exchange on the chemical shift time scale and was assigned by reference to the spectra of the free protein. The peptide contains residues 57–69 of Xis, which has previously been implicated in cooperative interactions with INT-DBD$^{1-64}$. (*B*) Overlay of ^{15}N–^{1}H HSQC spectra recorded with differing amounts of added peptide. Crosspeaks in black correspond to the free protein, and crosspeaks that are purple, magenta, cyan, green, red, and blue were recorded at protein:peptide ratios of 1:1, 1:1.5, 1:2, 1:3, 1:5, and 1:10, respectively. The graphic shows that the backbone amide resonances of residues 34, 51, and 53–55 of INT-DBD$^{1-64}$ are significantly perturbed by the Xis peptide.

is in contact with the carboxyl-terminal tail of Xis in solution (Fig. 5*B*). In addition, several amide resonances proximal to this site are perturbed, including the backbone amides of residues 27, 31, 32, and 34, and the side-chain amide and guanidino groups of Asn-15 and Arg-30, respectively. These latter sites do not form a continuous surface and are located within the three-stranded β-sheet (Fig. 6*A*), suggesting that they may be perturbed indirectly by a subtle movement of the helix, which forms the primary interaction surface for the Xis peptide.

Discussion

It has been shown that residues 1–70 of Int contain all of the information for cooperative homotypic interactions between Int protomers bound at adjacent P′1,2,3 arm-type sites and for the heterotypic interactions between Int bound at the very weak P2 site and Xis bound at the adjacent X1 site (40, 41). The NMR solution structure of Int residues 1–64 (INT-DBD$^{1-64}$) revealed a three-stranded β-sheet that packs against an α-helix. The β-sheet was proposed to interact with the arm-type DNA site by analogy with the structurally similar Tn*916* amino-terminal domain complexed with its cognate DNA-binding site, but the
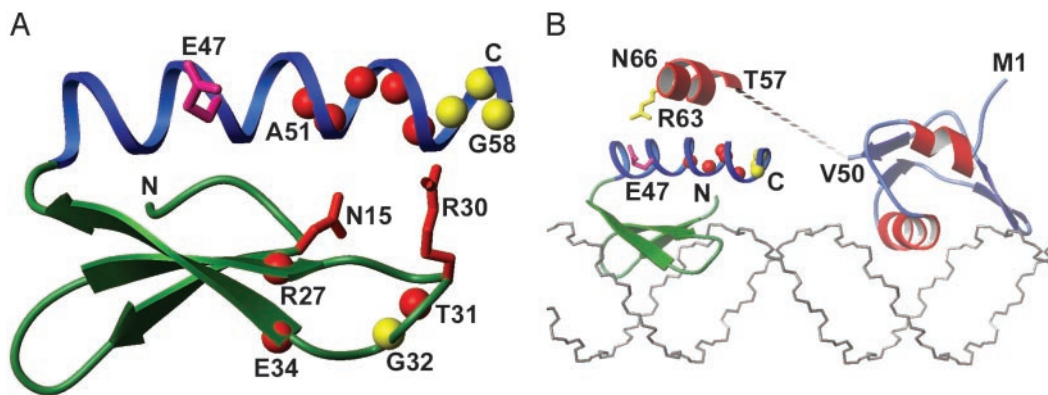
Fig. 6. The Xis peptide interacts with the carboxyl-terminal helix of INT-DBD$^{1-64}$. (*A*) A ribbon drawing of the INT-DBD$^{1-64}$ structure with backbone amide atoms that are affected by the Xis peptide indicated by spheres. Red and yellow spheres indicate significantly ($\Delta_{avg} > 0.15$) and modestly ($\Delta_{avg} = 0.1-0.15$) perturbed backbone amides, where Δ_{avg} is the weighted average chemical shift change ($\Delta_{avg} = \mathrm{sqrt}((\Delta\delta_{HN})^2 + (\Delta\delta_{N}\cdot0.17)^2)$). The side chains of Asn-15 and Arg-30 are perturbed by peptide and are red, and the side chain of Glu-47 implicated in Xis binding is pink. (*B*) Model of INT-DBD$^{1-64}$ and Xis bound to sites P2 and X1 within the *att*R attachment site. The structures of INT-DBD$^{1-64}$ and Xis solved in the absence of DNA (27, 28) were manually docked onto the duplex as described in the text. The positioning of INT-DBD$^{1-64}$ is based on the structure of related three-stranded β-sheet DNA-binding domains and projects E47 toward the carboxyl terminus of Xis for protein–protein interactions. The unstructured carboxyl-terminal tail of Xis (residues 52–72) is drawn as a dashed line, with the segment of the tail mimicked by the peptide used in the titration studies (residues 57–69) denoted by an α-helix placed proximal to the helix of INT-DBD$^{1-64}$. It should be noted that in a previous description of the structure (27), it was stated that the helix in INT-DBD$^{1-64}$ ended at residue L55, but it actually ends at residue G58.

role of the α-helix was not identified (27). A hydrophobic patch on the solvent-exposed face of the helix (I45, I49, and I53), and a mutation (R42L) in the analogous helix of the closely related Int from phage HK022 that seemed to enhance cooperative binding at P′1,2,3 (42), suggested this helix as a candidate surface for either of the two protein–protein interactions mediated by the amino-terminal domain.

The data reported here indicate that, in fact, both types of protein–protein interactions depend on a common site within the α-helix. The E47A mutation abolishes the formation of ternary complexes with Xis on the P2X1 DNA-binding sites (Fig. 3) and also diminishes the formation of ternary complexes involving two Int protomers at adjacent P′1,2 sites (Fig. 2). The relative magnitudes of the two different effects in electrophoretic mobility shift assays are mirrored by the properties of E47A Int in recombination: excisive recombination is virtually abolished, but only the rate of integrative recombination is affected. This phenotype is strikingly similar to that of a mutation (ts2268) isolated many years ago by Enquist and Weisberg (43), which failed to promote any recombination reaction that depended on Xis and was proficient for integrative recombination reactions that were not limited by time, i.e., prophage insertion and curing. However, in time-limited reactions, such as intermolecular recombinations between *att*P and *att*B, the mutant was clearly depressed relative to wild-type Int. It is interesting that ts2268 was the only one of a large screen of many mutants that had this unusual phenotype.

The suggestion of direct interactions between Int and Xis was made as early as the first purification of the Xis protein (44). More recently, the carboxyl-terminal tail residues of Xis (residues 52–72) have been specifically implicated in Int binding: challenge phage assays have indirectly shown the importance of residues T57, L60, R63, and I64 (29, 30) and electrophoretic mobility shift assays have directly demonstrated the importance of L60 and R63 (ref. 29 and this article). If these functionally significant residues were part of an α-helix, the side chains of L60, R63, and I64 would reside on the same helical surface. The role of an α-helix is further intimated by the finding that Xis amino acid substitutions that do not affect cooperative binding (K61, K62, and R65) are predicted to reside on the opposing helical surface. Because NMR studies have demonstrated the carboxyl-terminal tail of Xis is disordered in solution, the

available data strongly suggest that residues T57-I64 undergo a disordered to ordered transition to form a helix in the ternary complex. The helical interface with Int is expected to be largely hydrophobic and is presumably supplemented by a favorable electrostatic interaction(s) between R63 of Xis and E47 of Int. The E47 side chain is probably at the edge of this hydrophobic interface with its backbone amide sufficiently distant that a chemical shift perturbation is not observed. Indeed, the significant changes in the NMR spectra occur immediately adjacent to E47.

The available data suggest a model for the INT-DBD$^{1-64}$–Xis–DNA ternary complex (Fig. 6*B*). The proteins in the complex are predicted to bind to the same side of the duplex, with Xis positioned to insert its second helix (H2) and wing structures into the major and minor grooves, respectively, whereas the INT-DBD$^{1-64}$ is expected to place its three-stranded β-sheet near the adjacent major groove at site P2. This binding arrangement is consistent with previous modeling studies (28), extensive biochemical data (28, 30), and the presence of the winged helix–turn–helix and three-stranded β-sheet DNA-binding motifs in the Xis and INT-DBD$^{1-64}$ proteins, respectively (27, 28). Whereas previous work could not reliably predict the relative orientation of Xis and Int within the ternary complex, our NMR and mutagenesis studies now resolve this ambiguity, and strongly suggest that the proteins are situated to project their carboxyl-termini toward one another. This orientation enables potential helix–helix packing involving the side chains of I49 and I53 of INT-DBD$^{1-64}$ and L60 and I64 of Xis. Significantly, this orientation is compatible with the results of the NMR titration studies and the demonstrated importance of L60 and I64 of Xis (29, 30), E47 of Int (this article), and R63 of Xis (ref. 30 and this article).

In contrast to the structural and functional data highlighting Int residue E47, the role of Int residue R30 in Xis binding is much less clear. In the model, the DNA is B-form and the side chain of R30 does not contact Xis. However, in reality, the DNA in the ternary complex may be dramatically distorted enabling the highly basic carboxyl terminus of Xis to simultaneously contact E47 and R30. The aspartate substitution at R30 might thereby act to strengthen protein–protein interactions within this region and increase the affinity of the Int mutant for Xis in the ternary complex. However, it is also possible that the side chain of R30 does not directly contact Xis, and that the observed changes in

its NMR resonances result from subtle conformational changes that occur on peptide binding to the carboxyl-terminal helix of Int. In this scenario, the side chain of R30 could facilitate DNA binding, in the absence of Xis, to the P2 arm-type binding site. The putative destabilization of R30D binding to P2 would then be compensated by the formation of ternary complex with Xis (Fig. 3*A*). Because R30D exhibits enhanced formation of ternary complex and a two-fold depression of excisive recombination (data not shown), this finding leads to the interesting implication that an overly stable ternary complex at the P2X1 site might be detrimental for excisive recombination.

The dual role of residue E47 in heterotypic interactions with Xis and homotypic interactions between Ints bound at adjacent arm-type sites is especially interesting. In one model compatible with these results, Int uses the same helical surface for both kinds of protein–protein interactions: to enhance its binding at the very weak P2 site by interactions with Xis and to enhance its binding

at P′1,2,3 by interactions with an adjacent Int protomer. Such a model would be consistent with a mechanism that made integrative recombination very sensitive to the intracellular concentration of Int and excisive recombination even more sensitive to Xis binding at X1.

Note. While this work was being prepared for publication we learned that B. M. Swalla, E. H. Cho, R. I. Gumport, and J. F. Gardner (45) have sequenced and characterized the Int mutant ts2268 (E47K) and found it, and other E47 substitutions, to have similar properties to those described here for E47A.

1. Grainge, I. & Jayaram, M. (1999) *Mol. Microbiol.* **33,** 449–456.
2. Azaro, M. A. & Landy, A. (2002) in *Mobile DNA II*, eds. Craig, N. L., Craigie, R., Gellert, M. & Lambowitz, A. (Am. Soc. Microbiol., Washington, DC), pp. 118–148.
3. Ross, W. & Landy, A. (1982) *Proc. Natl. Acad. Sci. USA* **79,** 7724–7728.
4. Moitoso de Vargas, L., Pargellis, C. A., Hasan, N. M., Bushman, E. W. & Landy, A. (1988) *Cell* **54,** 923–929.
5. Moitoso de Vargas, L., Kim, S. & Landy, A. (1989) *Science* **244,** 1457–1461.
6. Richet, E., Abcarian, P. & Nash, H. A. (1988) *Cell* **52,** 9–17.
7. Craig, N. L. & Nash, H. A. (1984) *Cell* **39,** 707–716.
8. Thompson, J. F., Moitoso de Vargas, L., Skinner, S. E. & Landy, A. (1987) *J. Mol. Biol.* **195,** 481–493.
9. Thompson, J. F. & Landy, A. (1988) *Nucleic Acids Res.* **16,** 9687–9705.
10. Campbell, A. M. (1962) in *Advances in Genetics*, eds. Caspari, E. W. & Thoday, J. M. (Academic, New York), pp. 101–145.
11. Nash, H. A. (1974) *Nature* **247,** 543–545.
12. Hsu, P.-L. & Landy, A. (1984) *Nature* **311,** 721–726.
13. Nunes-Düby, S. E., Matsumoto, L. & Landy, A. (1987) *Cell* **50,** 779–788.
14. Numrych, T. E., Gumport, R. I. & Gardner, J. F. (1990) *Nucleic Acids Res.* **18,** 3953–3959.
15. Hickman, A. B., Waninger, S., Scocca, J. J. & Dyda, F. (1997) *Cell* **89,** 227–237.
16. Subramanya, H. S., Arciszewska, L. K., Baker, R. A., Bird, L. E., Sherratt, D. J. & Wigley, D. B. (1997) *EMBO J.* **16,** 5178–5187.
17. Guo, F., Gopaul, D. N. & Van Duyne, G. D. (1997) *Nature* **389,** 40–46.
18. Gopaul, D. N., Guo, F. & Van Duyne, G. D. (1998) *EMBO J.* **17,** 4175–4187.
19. Guo, F., Gopaul, D. N. & Van Duyne, G. D. (1999) *Proc. Natl. Acad. Sci. USA* **96,** 7143–7148.
20. Chen, Y., Narendra, U., Iype, L. E., Cox, M. M. & Rice, P. A. (2000) *Mol. Cell* **6,** 885–897.
21. Kostrewa, D., Granzin, J., Koch, C., Choe, H.-W., Labahn, J., Kahmann, R. & Saenger, W. (1991) *Nature* **349,** 178–180.
22. Kostrewa, D. (1992) *J. Mol. Biol.* **226,** 209–226.
23. Yuan, H. S., Finkel, S. E., Feng, J.-A., Kaczor-Grzeskowiak, M., Johnson, R. C. & Dickerson, R. E. (1991) *Proc. Natl. Acad. Sci. USA* **88,** 9558–9562.
24. Rice, P. A., Yang, S.-W., Mizuuchi, K. & Nash, H. A. (1996) *Cell* **87,** 1295–1306.
25. Kwon, H. J., Tirumalai, R. S., Landy, A. & Ellenberger, T. (1997) *Science* **276,** 126–131.
26. Aihara, H., Kwon, H. J., Nunes-Düby, S. E., Landy, A. & Ellenberger, T. (2003) *Mol. Cell*, in press.
27. Wojciak, J. M., Sarkar, D., Landy, A. & Clubb, R. T. (2002) *Proc. Natl. Acad. Sci. USA* **99,** 3434–3439.
28. Sam, M., Papagiannis, C., Connolly, K. M., Corselli, L., Iwahara, J., Lee, J., Phillips, M., Wojciak, J. M., Johnson, R. C. & Clubb, R. T. (2002) *J. Mol. Biol.* **324,** 791–805.
29. Numrych, T. E., Gumport, R. I. & Gardner, J. F. (1992) *EMBO J.* **11,** 3797–3806.
30. Wu, Z., Gumport, R. I. & Gardner, J. F. (1998) *J. Mol. Biol.* **281,** 651–661.
31. Tirumalai, R. S., Kwon, H., Cardente, E., Ellenberger, T. & Landy, A. (1998) *J. Mol. Biol.* **279,** 513–527.
32. Sambrook, J., Fritsch, E. F. & Maniatis, T. (1989) *Molecular Cloning* (Cold Spring Harbor Lab. Press, Plainview, NY).
33. Tirumalai, R. S., Healey, E. & Landy, A. (1997) *Proc. Natl. Acad. Sci. USA* **94,** 6104–6109.
34. Chong, S., Montello, G. E., Zhang, A., Cantor, E. J., Liao, W., Xu, M.-Q. & Benner, J. (1998) *Nucleic Acids Res.* **22,** 5109–5115.
35. Smith, P. K., Krohn, R. I., Hermanson, G. T., Mallia, A. K., Gartner, F. H., Provenzano, M. D., Fujimoto, E. K., Goeke, N. M., Olson, B. J. & Klenk, D. C. (1985) *Anal. Biochem.* **150,** 76–85.
36. Wiechelman, K. J., Braun, R. D. & Fitzpatrick, J. D. (1988) *Anal. Biochem.* **175,** 231–237.
37. Delaglio, F., Grzesiek, S., Vuister, G. W., Zhu, G., Pfeifer, J. & Bax, A. (1995) *J. Biomol. NMR* **6,** 277–293.
38. Johnson, B. A. & Blevins, R. A. (1994) *J. Biomol. NMR* **4,** 603–614.
39. Koradi, R., Billeter, M. & Wuthrich, K. (1996) *J. Mol. Graphics* **14,** 51–55.
40. Sarkar, D., Azaro, M. A., Aihara, H., Papagiannis, C., Tirumalai, R. S., Nunes-Düby, S. E., Johnson, R. C., Ellenberger, T. & Landy, A. (2002) *J. Mol. Biol.* **324,** 775–789.
41. Cho, E. H., Gumport, R. I. & Gardner, J. F. (2002) *J. Bacteriol.* **184,** 5200–5203.
42. Cheng, Q., Swalla, B. M., Beck, M., Alcaraz, R., Jr., Gumport, R. I. & Gardner, J. F. (2000) *Mol. Microbiol.* **36,** 424–436.
43. Enquist, L. W. & Weisberg, R. A. (1984) *Mol. Gen. Genet.* **195,** 62–69.
44. Abremski, K. & Gottesman, S. (1982) *J. Biol. Chem.* **257,** 9658–9662.
45. Swalla, B. M., Cho, E. H., Gumport, R. I. & Gardner, J. F. (2003) *Mol. Microbiol.*, in press.